

Small-Molecule Inhibitors of the TLR3/dsRNA Complex

Kui Cheng, Xiaohui Wang, and Hang Yin*

Department of Chemistry and Biochemistry, University of Colorado at Boulder, Boulder, Colorado 80309, United States

Supporting Information

ABSTRACT: The protein–RNA interface has been regarded as “undruggable” despite its importance in many biological processes. The toll-like receptor 3 (TLR3)/double-stranded RNA (dsRNA) complex provides an exciting target for a number of infectious diseases and cancers. We describe the development of a series of small-molecule probes that were shown to be competitive inhibitors of dsRNA binding to TLR3 with high affinity and specificity. In a multitude of assays, compound **4a** was profiled as a potent antagonist to TLR3 signaling and also repressed the expression of downstream signaling pathways mediated by the TLR3/dsRNA complex, including TNF- α and IL-1 β .

Interfering with protein–protein interactions or protein–nucleic acid interactions has been regarded as a daunting goal in drug discovery.¹ Major strides have been made during the past decade in developing small-molecule agents to target protein–protein interactions. However, regulation of protein–RNA interactions lags behind, arguably due to the fact that RNA molecules pose a particular challenge with their high flexibility.² RNA-binding proteins play key roles in post-transcriptional modifications, which, along with transcriptional regulation, is a main method of controlling gene expression during development. In the present study, we report novel molecular probes that disrupt double-stranded (ds) RNA binding to toll-like receptor 3 (TLR3) as a demonstration of the use of specific small-molecule agents to target the protein–RNA interface.

Toll-like receptors (TLRs) are highly conserved transmembrane proteins that detect pathogen-associated molecular patterns and elicit pathogen-specific immune responses.³ TLR3 signaling is activated by dsRNA released from necrotic cells during inflammation or viral infection.⁴ TLR3 activation induces secretion of type I interferons and pro-inflammatory cytokines, such as TNF- α , IL-1, and IL-6, triggering immune cell activation and recruitment that are protective during certain microbial infections.⁵ A dominant-negative TLR3 allele has been associated with increased susceptibility to herpes simplex encephalitis, a serious illness with significant risks of morbidity and death, upon primary infection with HSV-1 in childhood.⁶ In mice, TLR3 deficiency is associated with decreased survival upon coxsackie virus challenge.⁷ In addition, uncontrolled or sustained innate immune response via TLR3 has been shown to contribute to morbidity and mortality in certain viral infection models, including the West Nile disease, phlebovirus, vaccinia, and influenza A.^{8–11} Therefore, modulation of TLR3 pathways offers an attractive strategy to fight a variety of diseases.

Despite the significant potential, the discovery of small-molecule inhibitors of TLR3 has been slow due to the complexity associated with disrupting the protein–RNA contact: immense effort is required to design individual compounds that target specific RNA-binding domains with high binding affinity and selectivity.¹ Herein, we describe the successful identification and characterization of small-molecule probes for the TLR3/dsRNA complex.

In search of small-molecule probes, the 1.2 million-compound *Enamine* database was screened against the dsRNA-binding domain of TLR3 (crystal structure PDB: 3CIY¹²) using the Glide 5.6 program.¹³ Initially, nine hits (Figure 1) were selected for cell assay screening. Interestingly, almost all of the hits identified, with the exception of **T5528092**, from the *in silico* screening generally share the common motif of a D-amino acid conjugated with an aromatic substituent, implying a novel pharmacophore to target the RNA-binding site of TLR3.

These initial hits were first evaluated using our previously established high-throughput cell assay of TLR3 activation.¹⁴ A dsRNA, polyribonucleic:polyribocytidylic acid (Poly(I:C)), was employed to selectively activate TLR3 signaling, resulting in the activation of nitric oxide (NO) synthase and the production of NO in RAW 264.7 macrophage cells.¹⁵ We monitored the NO level as an indicator of Poly(I:C)-induced TLR3 activation to evaluate the drug's inhibitory activity.

Two compounds, **T5626448** and **T5260630** (shown in boxes in Figure 1), demonstrated mild inhibitory activities in whole cells, with IC₅₀ values of 154 \pm 6 and 145 \pm 4 μ M, respectively. Both of these two compounds are derivatives of D-phenylalanine, suggesting the D-phenylalanine backbone as the scaffold to develop small-molecule inhibitors of TLR3. Computational docking results also implied that **T5626448** and **T5260630** could be further optimized by varying the substituents on the benzene or thiophene rings (Supporting Information (SI), Figure S1).

With the hit compounds selected, we developed concise synthetic routes for both **T5626448** and **T5260630** (SI, Scheme S1), which allows an extensive structure–activity relationship (SAR) analysis. Various substitutions with different size and electron-withdrawing/donating capability were examined on the aromatic systems. To inspect the impact on the activities imposed by the stereogenic center, both *R*- and *S*-isomers were prepared.

An improvement of 2 orders of magnitude in inhibitory potency of **T5626448** was achieved, with compound **4a** (Figure 2A) showing a low micromolar (3.44 \pm 0.41 μ M) IC₅₀ value. By contrast, no significant activity improvement for

Received: December 15, 2010

Published: February 28, 2011

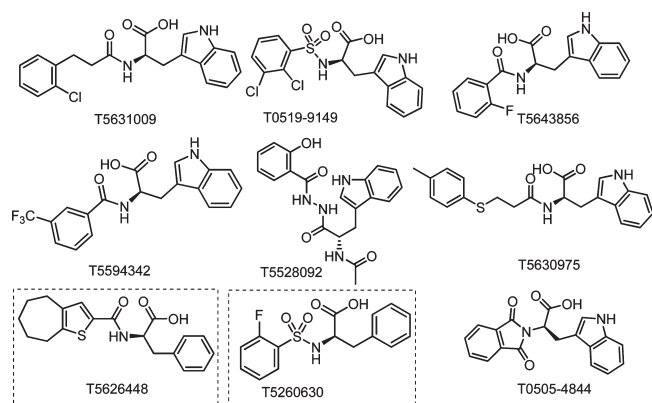


Figure 1. Chemical structures of the nine hits from the *in silico* screening of a 1.2 million-compound database, which imply a common structural motif.

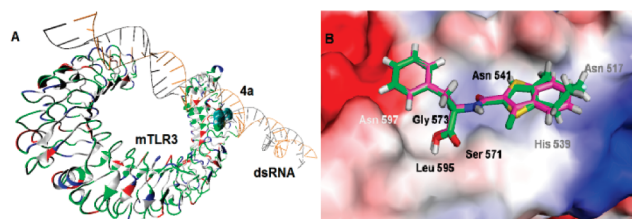


Figure 2. Molecular model of the identified compounds docked to TLR3. (A) Global view with the murine TLR3 binding to dsRNA, showing compound **4a** (shown in CPK representation) competing with dsRNA for the same binding site on the TLR3 surface. (B) Close-up view comparing the binding modes of **4a** (magenta) and **T5626448** (green) in complex with TLR3 (surface shown), indicating that the thiophene rings in the two compounds are flipped.

the **T5260630** derivatives was observed. Therefore, we decided to focus on the development of **T5626448** derivatives.

SAR studies of the **T5626448** derivatives lent support to the predicted binding mode of this series of TLR3 ligands (Table 1). First, substituting the seven-membered ring (**T5626448**) with a phenyl group decreased the inhibitory activity (**1a**, **1b**), suggesting that perhaps the benzene ring does not fit well into the hydrophobic pocket on the TLR3 surface. Therefore, we introduced some hydrophobic groups on the aromatic rings. With the replacement by smaller hydrophobic substituents, $-\text{CH}_3$ at the R_1 position and $-\text{Cl}$ at the R_2 position, the activity was increased significantly (**2a**, **2b**). Keeping $-\text{Cl}$ at the R_2 position and changing the R_1 substituent from $-\text{CH}_3$ to $-\text{Cl}$ or $-\text{F}$ (**3a**, **4a**) resulted in an increase of activity. It is noteworthy that the fluorine at R_1 and chlorine at the R_2 position promoted the potency significantly by nearly 45-fold (**4a**) compared to that of **T5626448**. Our docking results suggest that the elevated potency may be due to the fact that sulfur in **4a** is oriented in the opposite direction from that in **T5626448** (Figure 2B), which could facilitate hydrogen-bonding contacts with the TLR3 surface. Further, results demonstrate that an electron-withdrawing group is preferred at the R_1 position (**6a** vs **4a**). The $-\text{CF}_3$ replacement of $-\text{F}$ at the R_1 position decreased the activity slightly (**5a** vs **4a**), indicating that the electron density rather than the size is the dominating factor at this position. An additional hydroxyl group at the R_3 position greatly decreases the activity (**7a** vs **4a**), suggesting that higher hydrophobicity is favored at the amino

Table 1. Structure–Activity Relationship Analysis in RAW 264.7 Cells

compound	R_1	R_2	R_3	R_4	R_5	R_6	IC_{50} (μM) ^a
T5626448							154 ± 6
T5260630							145 ± 4
1a	$-\text{H}$	$-\text{H}$	$-\text{H}$	$-\text{H}$			>155
1b	$-\text{H}$	$-\text{H}$	$-\text{H}$	$-\text{H}$			>155
2a	$-\text{CH}_3$	$-\text{Cl}$	$-\text{H}$	$-\text{H}$			11.8 ± 1.3
2b	$-\text{CH}_3$	$-\text{Cl}$	$-\text{H}$	$-\text{H}$			31.7 ± 0.7
3a	$-\text{Cl}$	$-\text{Cl}$	$-\text{H}$	$-\text{H}$			5.60 ± 0.32
3b	$-\text{Cl}$	$-\text{Cl}$	$-\text{H}$	$-\text{H}$			11.8 ± 2.5
4a	$-\text{F}$	$-\text{Cl}$	$-\text{H}$	$-\text{H}$			3.44 ± 0.41
4b	$-\text{F}$	$-\text{Cl}$	$-\text{H}$	$-\text{H}$			21.9 ± 0.7
5a	$-\text{CF}_3$	$-\text{Cl}$	$-\text{H}$	$-\text{H}$			6.28 ± 1.05
5b	$-\text{CF}_3$	$-\text{Cl}$	$-\text{H}$	$-\text{H}$			19.8 ± 3.6
6a	$-\text{OCH}_3$	$-\text{Cl}$	$-\text{H}$	$-\text{H}$			36.7 ± 3.9
6b	$-\text{OCH}_3$	$-\text{Cl}$	$-\text{H}$	$-\text{H}$			>100
7a	$-\text{F}$	$-\text{Cl}$	$-\text{OH}$	$-\text{H}$			56.4 ± 5.2
7b	$-\text{F}$	$-\text{Cl}$	$-\text{OH}$	$-\text{H}$			84.7 ± 2.4
8a	$-\text{F}$	$-\text{Cl}$	$-\text{H}$	$-\text{F}$			70.7 ± 2.1
8b	$-\text{F}$	$-\text{Cl}$	$-\text{H}$	$-\text{F}$			79.5 ± 3.4
9a, 9b	$-\text{H}$	$-\text{H}$	$-\text{OH}$	$-\text{H}$			>100
10a, 10b	$-\text{H}$	$-\text{H}$	$-\text{H}$	$-\text{F}$			>100
11a, 11b	$-\text{H}$	$-\text{Cl}$	$-\text{H}$	$-\text{H}$			>100
12a	$-\text{H}$	$-\text{Cl}$	$-\text{H}$	$-\text{F}$			47.3 ± 4.1
12b	$-\text{H}$	$-\text{Cl}$	$-\text{H}$	$-\text{F}$			54.1 ± 5.7
13a, 13b	$-\text{F}$	$-\text{H}$	$-\text{H}$	$-\text{H}$			>100
14a, 14b					2-F	$-\text{H}$	>100
15a, 15b					3-F	$-\text{H}$	>100
16a, 16b					4-F	$-\text{H}$	>100
17a, 17b					2-F	$-\text{OH}$	>100
18a, 18b					3-F	$-\text{OH}$	>100
19a, 19b					4-F	$-\text{OH}$	>100

^a IC_{50} average values and corresponding SD values are determined from the results of at least three independent repeats.

acid side chain. With the absence of any substituent at the R_1 and the R_2 positions, the activity decreased significantly or was completely abolished (**9a–11a**, **13a**). Last, these **T5626448** derivatives' inhibitory effects are stereodependent, with the *R*-enantiomers generally demonstrating higher potency. In summary, we identified that compound **4a** shows dose-dependent inhibitory effects, blocking Poly(I:C)-induced TLR3 activation with an IC_{50} of $3.44 \pm 0.41 \mu\text{M}$ (Figure 3A). This low $\sim\mu\text{M}$ potency in whole cells is remarkable, given that the competing dsRNA is a tight binder to TLR3 ($K_d = 19 \pm 0.9 \text{ nM}$).¹⁶

A challenge in the development of inhibitors to target TLRs is to engineer specificity and potency. There are at least 12 homologous TLRs present in murine macrophages, all sharing a ligand-binding domain with a horseshoe shape.³ We therefore tested compound **4a** against a panel of homologous TLRs, including TLR1/2, TLR2/6, TLR3, TLR4, and TLR7, using TLR-specific

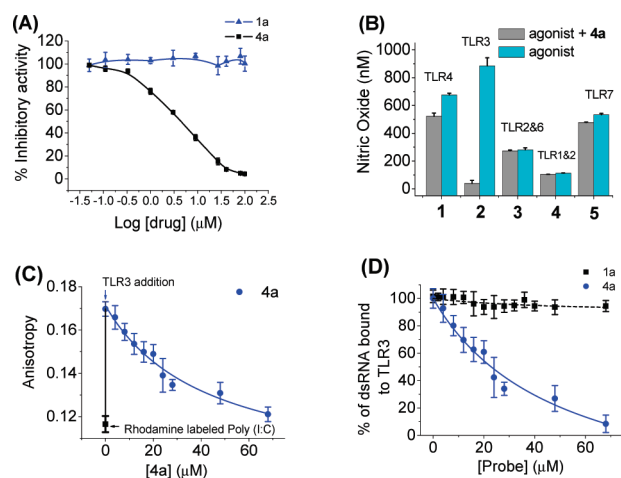


Figure 3. (A) Dose-dependent inhibitory response of Poly(I:C)-induced TLR3 activation by **4a** and **1a** (negative control). (B) Specificity test for **4a** (27 μM) with TLR-specific agonists used to selectively activate the respective TLRs: (1) TLR4, 10 ng/mL LPS; (2) TLR3, 15 μg/mL Poly(I:C); (3) TLR2/6, 10 ng/mL FSL-1; (4) TLR1/2, 200 ng/mL Pam₃CSK₄; and (5) TLR7, 100 nM R848. (C) Fluorescence anisotropy assay, showing competitive binding between **4a** and dsRNA ($K_d = 19 \pm 0.9$ nM) for TLR3. The inhibition curve was fitted using a one-site competition model. (D) Normalized binding of **4a** compared with the negative control, **1a**.

ligands to selectively activate a particular TLR signaling pathway. We found that **4a** inhibits TLR3 signaling without affecting other TLRs, showing it is highly selective in intact cells (Figure 3B). Further, compound **4a** was found to have low cytotoxicity. CYP450 tests showed that **4a** did not affect a panel of cytochrome enzymes (CYP3A4, 2D6, 2C19, and 1A2) (SI, Figure S2). The low toxicity of **4a** was further confirmed in RAW 264.7 cells using the established WST-1 methodology (SI, Figure S3). Last, kinase profiling showed that compound **4a** demonstrated negligible inhibition activity against a panel of 12 representative kinases (SI, Figure S4).

Biophysical tests were carried out for **4a**, along with the negative control compound **1a**, to demonstrate that **4a** directly binds to TLR3. Fluorescence anisotropy assays showed that **4a** competes with dsRNA for binding to TLR3 with $K_i = 2.96 \pm 0.32$ μM, which is consistent with its potency observed in the whole cell assay. The anisotropy of rhodamine-labeled Poly(I:C) showed a robust increase from 0.116 to 0.171 (Figure 3C) upon addition of TLR3 (excitation, 546 nm; emission, 576 nm). This increase is consistent with the anisotropy changes seen with ligand–receptor pairs of comparable sizes.¹⁷ Increasing **4a**'s concentration to 68 μM decreased the anisotropy to background levels, presumably due to release of the fluorescently labeled Poly(I:C) probe (Figure 3D). These data were then fitted to a one-site-competition model. Good fitting ($R^2 > 0.98$) confirmed that **4a** and dsRNA compete for the same binding site on the TLR3 surface. Taken together, these results support that **4a** disrupts the TLR3/dsRNA association by directly targeting the RNA-binding site on TLR3.

Last, we used a secondary cellular assay to confirm that **4a** also inhibits the downstream signaling transduction mediated by the formation of the TLR3/dsRNA complex. In addition to TLR3 signaling suppression, the release of the pro-inflammatory cytokines, TNF-α and IL-1β, was investigated. The results (Figure 4) showed that **4a** almost completely abolishes the TLR3-mediated

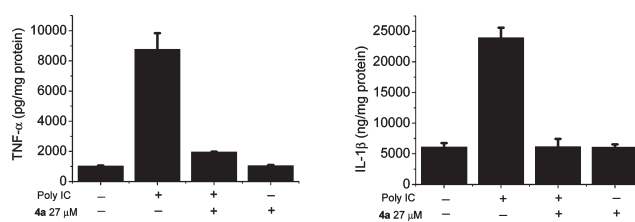


Figure 4. ELISA assay results showed that **4a**, at its IC₉₀ concentration (27 μM), abolishes the TNF-α and IL-1β production activated by 15 μg/mL Poly (I:C) in the RAW 264.7 cells.

inflammation response at its IC₉₀ concentration (27 μM). The inhibitory effects of TNF-α by **4a** at 10 μM were also tested. Approximately 60% inhibition was observed, agreeing with the results observed in the NO synthase assay (SI, Figure S5). Taken together, these results suggest that **4a** suppresses the downstream signaling of TLR3 in a consistent manner in which it disrupts the TLR3/dsRNA complex formation.

In conclusion, we have successfully selected a series of novel small-molecule inhibitors targeting the dsRNA binding region of TLR3 with high specificity and binding affinity both *in vitro* and in whole cells. Compound **4a** provides a much needed molecular probe for studying protein–RNA interactions. In general, this effective method will shed light on the future design of potent and selective molecular probes for RNA-binding proteins, which may facilitate studies of highly important protein–RNA complexes.

■ ASSOCIATED CONTENT

S Supporting Information. Full details of the *in silico* virtual screening, full characterization of the individual compounds examined, and complete ref 6. This material is available free of charge via the Internet at <http://pubs.acs.org>.

■ AUTHOR INFORMATION

Corresponding Author

hang.yin@colorado.edu

■ ACKNOWLEDGMENT

We thank the National Institutes of Health (DA026950, DA025740, NS067425, RR025780, and DA029119) for financial support of this work. K.C. is supported by a visiting student scholarship from the China Scholarship Council (Grant No. 2009619072). We thank Dr. Sherry A. Chavez, Dr. Peter Brown, and Alexander J. Martinko for their comments on the manuscript.

■ REFERENCES

- (1) (a) Boger, D. L.; Desharnais, J.; Capps, K. *Angew. Chem. Int. Ed.* **2003**, *42*, 4138. (b) Yin, H.; Hamilton, A. D. *Angew. Chem. Int. Ed.* **2005**, *44*, 4130.
- (2) (a) Jinek, M.; Doudna, J. A. *Nature* **2009**, *457*, 405. (b) Sashital, D. G.; Doudna, J. A. *Curr. Opin. Struct. Biol.* **2010**, *20*, 90.
- (3) Takeuchi, O.; Akira, S. *Cell* **2010**, *140*, 805.
- (4) Oshiumi, H.; Matsumoto, M.; Funami, K.; Akazawa, T.; Seya, T. *Nat. Immunol.* **2003**, *4*, 161.
- (5) Barton, G. M.; Medzhitov, R. *Science* **2003**, *300*, 1524.
- (6) Zhang, S. Y.; et al. *Science* **2007**, *317*, 1522.
- (7) Richer, M. J.; Lavallée, D. J.; Shanina, I.; Horwitz, M. S. *PLoS One* **2009**, *4*, e4127.

- (8) Wang, T.; Town, T.; Alexopoulou, L.; Anderson, J. F.; Fikrig, E.; Flavell, R. A. *Nat. Med.* **2004**, *10*, 1366.
- (9) Gowen, B. B.; Hoopes, J. D.; Wong, M. H.; Jung, K. H.; Isakson, K. C.; Alexopoulou, L.; Flavell, R. A.; Sidwell, R. W. *J. Immunol.* **2006**, *177*, 6301.
- (10) Hutchens, M.; Luker, K. E.; Sottile, P.; Sonstein, J.; Lukacs, N. W.; Núñez, G.; Curtis, J. L.; Luker, G. D. *J. Immunol.* **2008**, *180*, 483.
- (11) Pashine, A.; Valiante, N. M.; Ulmer, J. B. *Nat. Med.* **2005**, *11*, S63.
- (12) Liu, L.; Botos, I.; Wang, Y.; Leonard, J. N.; Shiloach, J.; Segal, D. M.; Davies, D. R. *Science* **2008**, *320*, 379.
- (13) (a) *Glide*, version 5.6; Schrödinger, LLC: New York, NY, 2010. (b) Halgren, T. A.; Murphy, R. B.; Friesner, R. A.; Beard, H. S.; Frye, L. L.; Pollard, W. T.; Banks, J. L. *J. Med. Chem.* **2004**, *47*, 1750.
- (14) (a) Bevan, D. E.; Martinko, A. J.; Loram, L. C.; Stahl, J. A.; Taylor, F. R.; Joshee, S.; Watkins, L. R.; Yin, H. *ACS Med. Chem. Lett.* **2010**, *1*, 194. (b) Joce, C. M.; Stahl, J. A.; Shridhar, M.; Hutchinson, M. R.; Watkins, L. R.; Fedichev, P. O.; Yin, H. *Bioorg. Med. Chem. Lett.* **2010**, *20*, 5411.
- (15) Heitmeier, M. R.; Scarim, A. L.; Corbett, J. A. *J. Biol. Chem.* **1998**, *273*, 15301.
- (16) Fukuda, K.; Watanabe, T.; Tokisue, T.; Tsujita, T.; Nishikawa, S.; Hasegawa, T.; Seya, T.; Matsumoto, M. *J. Biol. Chem.* **2008**, *283*, 22787.
- (17) Xu, H. Q.; Zhang, A. H.; Auclair, C.; Xi, X. G. *Nucleic Acids Res.* **2003**, *31*, e70.